

# Evaluation and comparison of FEM and BEM for extraction of homogeneous substrates

**Citation for published version (APA):**

Ugryumova, M., & Schilders, W. H. A. (2011). *Evaluation and comparison of FEM and BEM for extraction of homogeneous substrates*. (CASA-report; Vol. 1108). Technische Universiteit Eindhoven.

**Document status and date:**

Published: 01/01/2011

**Document Version:**

Publisher's PDF, also known as Version of Record (includes final page, issue and volume numbers)

**Please check the document version of this publication:**

- A submitted manuscript is the version of the article upon submission and before peer-review. There can be important differences between the submitted version and the official published version of record. People interested in the research are advised to contact the author for the final version of the publication, or visit the DOI to the publisher's website.
- The final author version and the galley proof are versions of the publication after peer review.
- The final published version features the final layout of the paper including the volume, issue and page numbers.

[Link to publication](#)

**General rights**

Copyright and moral rights for the publications made accessible in the public portal are retained by the authors and/or other copyright owners and it is a condition of accessing publications that users recognise and abide by the legal requirements associated with these rights.

- Users may download and print one copy of any publication from the public portal for the purpose of private study or research.
- You may not further distribute the material or use it for any profit-making activity or commercial gain
- You may freely distribute the URL identifying the publication in the public portal.

If the publication is distributed under the terms of Article 25fa of the Dutch Copyright Act, indicated by the "Taverne" license above, please follow below link for the End User Agreement:

[www.tue.nl/taverne](http://www.tue.nl/taverne)

**Take down policy**

If you believe that this document breaches copyright please contact us at:

[openaccess@tue.nl](mailto:openaccess@tue.nl)

providing details and we will investigate your claim.

**EINDHOVEN UNIVERSITY OF TECHNOLOGY**  
Department of Mathematics and Computer Science

CASA-Report II-08  
February 2011

Evaluation and comparison of FEM and BEM  
for extraction of homogeneous substrates

by

M.V. Ugryumova, W.H.A. Schilders



Centre for Analysis, Scientific computing and Applications  
Department of Mathematics and Computer Science  
Eindhoven University of Technology  
P.O. Box 513  
5600 MB Eindhoven, The Netherlands  
ISSN: 0926-4507



# Evaluation and Comparison of FEM and BEM for Extraction of Homogeneous Substrates

M. V. Ugryumova, W. H. A. Schilders

<sup>1</sup> Department of Mathematics and Computer Science of Eindhoven University of Technology, Eindhoven, The Netherlands (phone: 31-40-2478388; e-mail: m.v.ugryumova@tue.nl).

## SUMMARY

In the design and fabrication of micro-electronic circuits, it is necessary to simulate and predict many kinds of effects, such as substrate crosstalk, interconnect delays and others. In order to simulate and predict properly these effects, accurate and efficient substrate modeling methods are required. Substrate resistance extraction involves finding a resistance network between ports correctly describing the behaviour of the substrate. In this report we consider the problem of resistance extraction of a substrate with a homogeneous doping profile. We solve the problem by means of two discretization methods, namely the finite element method (FEM) and the boundary element method (BEM) and discuss the advantages and disadvantages of each of these methods. We particularly addresses the problem of achieving grid-independent results and characterize the cases in which one technique is better than the other.

## 1. INTRODUCTION

Nowadays digital technologies operate with frequencies of the order of gigahertz (GHz). This results into non-negligible delays and field couplings which may be critical for an integrated circuit (IC) performance. Figure 1 schematically shows a vertical cross section of an IC. It consists of three layers: interconnect layout, layout with devices, and substrate. Ideally interconnect is an ideal conductor, devices (transistors, diodes) are ideal switches, and substrate is an ideal insulator. However when operating at high frequencies, interconnect causes delays, and therefore it cannot be treated as an ideal conductor; transistors are not ideal switches; and the substrate may cause crosstalk between different parts of the IC. This non-ideal behaviour is called *parasitics*.

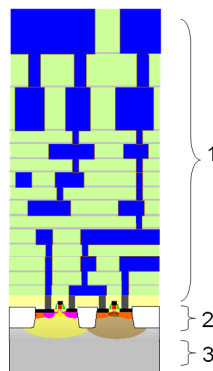


Figure 1. Layers of IC: 1. interconnect, 2. devices, 3. substrate

At low frequencies these parasitic effects are usually negligible, because switching delay in the transistors and delays along the interconnect are much smaller in comparison to the speed of the

signal [14]. Therefore, to simulate and predict properly impact of parasitic effects, accurate and efficient modeling methods are required.

To exploit the underlying physics of IC one can subdivide the whole modeling problem of IC into three subproblems: modeling of interconnect, modeling of devices, and modeling of substrate. We recall that modeling of interconnect [1][13] and devices [7] is a field of research on its own, and it is out of the scope of this report. In this report we discuss the problem of modeling of homogeneous substrates. We study the advantages and disadvantages of the popular discretization methods, namely FEM and BEM, and compare them on the qualitative level. We particularly addresses the problem of achieving grid-independent results and characterize the cases in which one technique is better than the other.

This report is build up as follows. In Section 2 we derive the Laplace equation from the Maxwell's equations and present a corresponding boundary value problem which has to be solved in order to obtain a resistance network. In Sections 3 and 4 we review FEM and BEM and show construction of corresponding conductance matrices which describe the resistive network by each method. Then, comparison of both methods for a 2D substrate is considered in Section 5, while comparison for a 3D case is presented in Section 6. We specially put emphasis on discretization and the problem of obtaining grid-independent results.

## 2. MODELING OF SUBSTRATE

Semiconductor behaviour can be described by the semiconductor equations which are mostly relevant for the modeling of devices. Nevertheless the global characteristics of the substrate can be captured with sufficient accuracy by taking into account dominant factors of the semiconductor behaviour. In this report the modeling approach is aimed at modeling the global behaviour of a homogeneous substrate and therefore does not take into account the full semiconductor equations.

The Maxwell's equations for harmonic fields are given by [11]

$$\nabla \times \mathbf{E} = i\omega\mathbf{B} \quad (\text{Faraday's law}), \quad (1)$$

$$\nabla \times \mathbf{H} = \mathbf{J} - i\omega\mathbf{D} \quad (\text{Ampere's law}), \quad (2)$$

$$\nabla \cdot \mathbf{B} = 0 \quad (\text{Gauss's law}), \quad (3)$$

$$\nabla \cdot \mathbf{D} = \rho, \quad (4)$$

where  $\mathbf{E}$  is the electric field,  $\mathbf{H}$  is the magnetic field,  $\mathbf{B}$  is the magnetic induction,  $\mathbf{D}$  is the electric displacement,  $\mathbf{J}$  is the current density,  $\rho$  is the charge density. Associated with the Maxwell's equations, we have a continuity equation:

$$\nabla \cdot \mathbf{J} - i\omega\rho = 0. \quad (5)$$

We consider linear, homogenous, and isotropic media, such that

$$\mathbf{D} = \epsilon\mathbf{E}, \quad \mathbf{B} = \mu\mathbf{H}, \quad \mathbf{J} = \sigma\mathbf{E},$$

where the scalars  $\epsilon$  (permittivity),  $\mu$  (permeability) and  $\sigma$  (conductivity) are assumed to be constant.

Since describing the substrate via the Maxwell's equations (1)–(4) is unnecessary complicated, we consider the following assumptions [14]: 1) the fields are quasi-static, 2) the domain does not contain fixed charges or current sources, and 3) the domain is assumed to be purely conductive.

The quasi-static assumption means that the electric and magnetic fields are highly localized within the circuit elements [17]. Although the electric displacement  $\mathbf{D}$  is dominant within a capacitor, it is negligible outside, so that Ampere's law (2) can neglect variations of  $\mathbf{D}$  making the current divergence free, i.e.,

$$\nabla \cdot \mathbf{J} = 0. \quad (6)$$

This means that the algebraic sum of all currents flowing into or out of a node is zero, which is Kirchhoff's current law. Similarly, variations of magnetic induction  $\mathbf{B}$  in (1) is assumed negligible

outside of inductors, so the electric field is curl free, i.e.,  $\nabla \times \mathbf{E} = 0$ . In fact this is Kirchoff's voltage law that the algebraic sum of voltage drops is zero, i.e.,

$$\mathbf{E} = -\nabla u, \quad (7)$$

where  $u$  denotes the potential.

### 2.1. Mathematical formulation of the problem

An example of a substrate is shown in Figure 2. It consists of a domain  $\Omega$  with a conductivity  $\sigma$ , and ideally conducting terminals (black quadrilateral elements) on top of the substrate. Boundary of the substrate includes terminal areas ( $\Gamma_1$ ) and non-terminal area ( $\Gamma_2$ ).

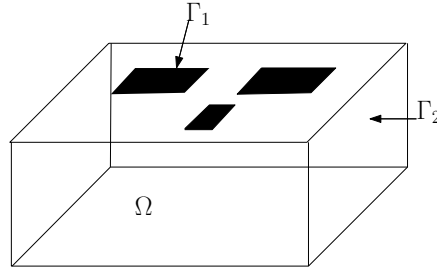


Figure 2. A substrate with three contacts on the top.

To derive the Laplace equation, we note that a distributed formulation of the Ohm's law can be written as

$$\mathbf{J} = \sigma \mathbf{E}. \quad (8)$$

Substituting (7) into (8) and substituting the result into (6), we obtain the following differential equation

$$\nabla \cdot (\sigma \nabla u) = 0. \quad (9)$$

If the conductivity in the domain is homogeneous, i.e.,  $\sigma$  is constant, then (9) becomes the Laplace equation

$$\sigma \nabla^2 u = 0. \quad (10)$$

Since we have to find a resistive network which describes a homogeneous substrate, one has to solve the Laplace equation with appropriate boundary conditions. The boundary conditions are chosen such that current can enter or leave the domain through the contact areas while remaining boundary has insulating properties. This requires to define Dirichlet boundary conditions on the contact areas, i.e.,

$$u = \bar{u} \quad \text{on} \quad \Gamma_1, \quad (11)$$

and homogeneous Neumann boundary conditions on the remaining boundary, i.e.,

$$\frac{\partial u}{\partial \mathbf{n}} = \bar{q} = 0 \quad \text{on} \quad \Gamma_2, \quad (12)$$

where  $\mathbf{n}$  is the normal to the boundary  $\Gamma = \Gamma_1 \cup \Gamma_2$  (note that  $\Gamma_1 \cap \Gamma_2 = \emptyset$ ). There is a connection between  $\frac{\partial u}{\partial \mathbf{n}}$  and the normal component of the current density,  $J_n$ , through the contact:

$$J_n = \sigma \frac{\partial u}{\partial \mathbf{n}} \quad \text{on} \quad \Gamma_2. \quad (13)$$

Homogenous Neumann boundary condition implies that  $J_n = 0$ , i.e., no current flowing through the boundary  $\Gamma_2$ . Extraction of the network requires to solve the Laplace equation with the above boundary conditions. Further we will consider two methods to solve the Laplace equation: FEM and BEM. We will compare both methods on a qualitative level.

## 3. THE FINITE ELEMENT METHOD

FEM is a popular technique for substrate modeling [6][2]. We will solve the 2D boundary value problem (9)–(12) by FEM and show the process of extraction of resistance network. First, we construct the weak formulation of the problem by defining the weighted residual of (10) for a single element with domain  $\Omega_h$ . The element residual takes the form:

$$r_h = \sigma \left( \frac{\partial^2 u}{\partial x^2} + \frac{\partial^2 u}{\partial y^2} \right).$$

Since the numerical solution  $u$  is generally not identical to the exact solution,  $r_h$  is nonzero. Our objective is to minimize  $r_h$  in a weighted sense. To achieve this, we first multiply  $r_h$  with a weighted function  $\omega$ , then integrate the result over the area of the element, and then set the integral to zero:

$$\sigma \int_{\Omega_h} \omega \left( \frac{\partial^2 u}{\partial x^2} + \frac{\partial^2 u}{\partial y^2} \right) d\Omega_h = 0. \quad (14)$$

Taking into account that  $\omega \frac{\partial^2 u}{\partial x^2} = \frac{\partial}{\partial x} \left( \omega \frac{\partial u}{\partial x} \right) - \frac{\partial \omega}{\partial x} \frac{\partial u}{\partial x}$ , (14) can be rewritten as

$$\sigma \int_{\Omega_h} \left( \frac{\partial}{\partial x} \left( \omega \frac{\partial u}{\partial x} \right) + \frac{\partial}{\partial y} \left( \omega \frac{\partial u}{\partial y} \right) \right) d\Omega_h - \sigma \int_{\Omega_h} \left( \frac{\partial \omega}{\partial x} \frac{\partial u}{\partial x} + \frac{\partial \omega}{\partial y} \frac{\partial u}{\partial y} \right) d\Omega_h = 0. \quad (15)$$

The Green's theorem states that the area integral of the divergence of a vector quantity equals to the total outward flux of the vector quantity through the contour that bounds the area, i.e.,

$$\int_{\Omega_h} \left( \frac{\partial A_x}{\partial x} + \frac{\partial A_y}{\partial y} \right) d\Omega_h = \oint_{\Gamma_h} (A_x + A_y) \cdot \mathbf{a}_n dl,$$

where  $\mathbf{a}_n = a_x \mathbf{n}_x + a_y \mathbf{n}_y$  is the outward unit vector that is normal to the boundary of the element. Applying Green's theorem to the first integral of (15), one obtains:

$$\int_{\Omega_h} \left( \frac{\partial \omega}{\partial x} \frac{\partial u}{\partial x} + \frac{\partial \omega}{\partial y} \frac{\partial u}{\partial y} \right) d\Omega_h = \oint_{\Gamma_h} \omega \left( \frac{\partial u}{\partial x} \mathbf{n}_x + \frac{\partial u}{\partial y} \mathbf{n}_y \right) dl. \quad (16)$$

According to Galerkin approach, the weight function  $\omega$  must belong to the same set of basis functions that are used to interpolate  $u$ . In general we interpolate  $u$  with the set of Lagrange polynomials as

$$u = \sum_{i=1}^n N_i(x, y) u_i^e, \quad (17)$$

where  $N_j$  are the corresponding basis functions based on Lagrange polynomials (interpolation functions),  $n$  is the number of local nodes per element, and  $u_i^e$  are unknown coefficients at a single mesh element. Substituting (17) into (16), and setting

$$\omega = N_i, \quad i = 1, \dots, n$$

the weak form of the differential equation becomes

$$\int_{\Omega_h} \left( \frac{\partial N_i}{\partial x} \sum_{j=1}^n u_j^e \frac{\partial N_j}{\partial x} + \frac{\partial N_i}{\partial y} \sum_{j=1}^n u_j^e \frac{\partial N_j}{\partial y} \right) d\Omega_h = \oint_{\Gamma_h} N_i \left( \frac{\partial u}{\partial x} \mathbf{n}_x + \frac{\partial u}{\partial y} \mathbf{n}_y \right) dl, \quad i = 1, \dots, n,$$

and can be rewritten in the matrix form as follows

$$Y_h \mathbf{u}_h = \mathbf{i}_h, \quad (18)$$

where

$$Y_{h,ij} = \int_{\Omega_h} \left( \frac{\partial N_i}{\partial x} \frac{\partial N_j}{\partial x} + \frac{\partial N_i}{\partial y} \frac{\partial N_j}{\partial y} \right) d\Omega_h, \quad (19)$$

$$\mathbf{u}_h = ( u_{h,1} \quad \dots \quad u_{h,n} )^T, \quad (20)$$

$$\mathbf{i}_{h,i} = \oint_{\Gamma_h} N_i \left( \frac{\partial u}{\partial x} \mathbf{n}_x + \frac{\partial u}{\partial y} \mathbf{n}_y \right) d\Omega_h, \quad i, j = 1, \dots, n. \quad (21)$$

The above  $Y_h$ ,  $\mathbf{u}_h$  and  $\mathbf{i}_h$  correspond to a stamp which represents a single finite element. For example, if the finite element is triangular with linear basis functions,  $Y_h$  becomes 3 by 3 matrix and vector  $\mathbf{u}_h$  (unknown) defines three voltages at the nodes of the element. If finite element has no edges at the boundary, then integral (21) equals zero. This follows from the conservation current law which states that  $\oint_{\Gamma_h} \mathbf{n} \cdot \mathbf{J} dl = \int_{\Omega_h} \nabla \cdot \mathbf{J} ds = 0$ . The linear basis functions imply that each edge in the FEM discretization is equivalent to a resistance network which is schematically presented in Figure 3.

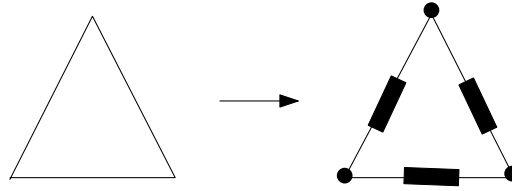


Figure 3. Left triangular from FEM discretization represents resistance network on the right.

To evaluate the integrals in (19) and (21), it is necessary to change the variables of integration. In other words, instead of integrating over the triangular element on the regular coordinate system, it is more convenient that the integration is carried out on the master triangle which lies on the natural coordinate system. Details about evaluating integral (19) for linear triangular elements can be found, for instance, in [6][12].

Based on the stamp data for a single element, the global matrix of the whole domain  $\Omega$  can be constructed. Let  $N$  denote the number of nodes in the global discretization. In this case one can define a system

$$Y\mathbf{U} = \mathbf{I}, \quad (22)$$

where  $Y \in \mathbb{R}^{N \times N}$  is symmetric matrix with elements defined in (19),  $\mathbf{I} \in \mathbb{R}^N$  contains elements defined in (21), and  $\mathbf{U} \in \mathbb{R}^N$  denotes vector of potentials at the nodes. Note, that for interior edges of finite elements the contribution of (21) is zero.

Since in triangular mesh, each element interacts only with neighboring elements, not all entries of  $Y$  are filled, which makes  $Y$  a sparse matrix. Therefore the resulting resistance network is large and sparse. However, only a small number of FEM nodes belong to the contact areas, while the rest of FEM nodes are internal nodes. Since internal nodes are not connected to other physical structures, then the FEM network has to be solved such that the internal nodes are eliminated and only the nodes at the contacts remain. Below we show how it can be done.

**3.0.1. Conductance matrix** Since not all nodes belong to the contact areas, we subdivide all nodes into two subsets. The first subset includes nodes at the contacts, i.e., external nodes or ports (index  $p$ ), the second subset includes all other nodes, i.e., internal nodes (index  $i$ ). Thus, we rewrite equation (22) in a block matrix form as

$$\begin{pmatrix} Y_{11} & Y_{12} \\ Y_{21} & Y_{22} \end{pmatrix} \begin{pmatrix} \mathbf{U}_p \\ \mathbf{U}_i \end{pmatrix} = \begin{pmatrix} \mathbf{I}_p \\ \mathbf{I}_i \end{pmatrix}, \quad (23)$$

where  $Y_{11} \in \mathbb{R}^{N_p \times N_p}$ ,  $Y_{12} \in \mathbb{R}^{N_p \times N_i}$ , and  $Y_{22} \in \mathbb{R}^{N_i \times N_i}$ ,  $N_p$  denotes the number of nodes located at the contacts, and  $N_i$  denotes the number of remaining nodes. To define a total potential at each contact area, we introduce an incidence matrix  $F \in \{1, -1, 0\}^{N_p \times N_c}$  ( $N_c$  is the number of contacts)



as follows [6]

$$F_{ij} = \begin{cases} 1 & \text{if node } i \text{ is on terminal } j \\ 0 & \text{otherwise.} \end{cases}$$

Let  $\mathbf{U}_c \in \mathbb{R}^{N_c}$  denote potentials at the contact areas, and  $\mathbf{U}_i \in \mathbb{R}^{N_i}$  denote potentials at the nodes located outside of the contacts. Then (23) can be rewritten as

$$\begin{pmatrix} F^T Y_{11} F & F^T Y_{12} \\ Y_{21} F & Y_{22} \end{pmatrix} \begin{pmatrix} \mathbf{U}_c \\ \mathbf{U}_i \end{pmatrix} = \begin{pmatrix} \mathbf{I}_c \\ \mathbf{0} \end{pmatrix}, \quad (24)$$

where  $\mathbf{I}_c \in \mathbb{R}^{N_c}$  is a total current at the contacts. Eliminating  $\mathbf{U}_i$  one obtains

$$\mathbf{I}_c = \underbrace{(F^T Y_{11} F - F^T Y_{12} Y_{22}^{-1} Y_{21} F)}_{G_s} \mathbf{U}_c,$$

where  $G_s$  is symmetric positive semidefinite conductance matrix which contains total path resistances of the resistance network.

#### 4. THE BOUNDARY ELEMENT METHOD

We will solve the 2D boundary value problem (10)–(12) by BEM and show the process of extraction of resistance network. BEM is based on an integral form of the Laplace equation [3][16]. Taking into account Dirichlet and Neumann boundary conditions, the integral form of the Laplace equation has the form

$$\int_{\Omega} (\nabla^2 u) \omega d\Omega - \int_{\Gamma_2} \left( \frac{\partial u}{\partial \mathbf{n}} - \bar{q} \right) \omega d\Gamma + \int_{\Gamma_1} (u - \bar{u}) \frac{\partial \omega}{\partial \mathbf{n}} d\Gamma = 0, \quad (25)$$

where  $\omega$  denotes an arbitrary weighting function which is continuous up to the second derivative. Further we will choose  $\omega$  equal to the Green's function. The Green's function  $G(p, q)$  is a fundamental solution of the Laplace equation:

$$\nabla^2 G(p, q) + \Delta^p = 0, \quad (26)$$

where  $\Delta^p$  represents a Dirac Delta function which tends to infinity at the point  $x = x^p$  and is equal to zero anywhere else. The Green's function  $G(p, q)$  can be viewed as the function describing the potential at a position  $p$ , resulting from a unit point charge placed at position  $q$ . For the 2D homogeneous case of the Laplace equation, the Green's function is

$$G(p, q) = \frac{1}{2\pi} \ln \frac{1}{r},$$

and for the 3D case

$$G(p, q) = \frac{1}{4\pi r},$$

where  $r = |p - q|$ . Let the weighting function  $\omega$  be chosen as the Green's function. Substituting  $\omega = G(p, q)$  into (25), and integrating by parts twice, we obtain

$$\int_{\Omega} (\nabla^2 G) u d\Omega = \int_{\Gamma_2} u \frac{\partial G}{\partial \mathbf{n}} d\Gamma_2 - \int_{\Gamma_2} \bar{q} G d\Gamma_2 - \int_{\Gamma_1} \frac{\partial u}{\partial \mathbf{n}} G d\Gamma_1 + \int_{\Gamma_1} \bar{u} \frac{\partial G}{\partial \mathbf{n}} d\Gamma_1. \quad (27)$$

From (26) it follows that

$$\int_{\Omega} (\nabla^2 G(p, q)) u d\Omega = - \int_{\Omega} \Delta^p u d\Omega = -u^p. \quad (28)$$

Substituting (28) into (27) we obtain

$$\alpha u^p = - \int_{\Gamma_2} u \frac{\partial G}{\partial \mathbf{n}} d\Gamma_2 + \int_{\Gamma_2} \bar{q} u d\Gamma_2 + \int_{\Gamma_1} \frac{\partial u}{\partial \mathbf{n}} G d\Gamma_1 - \int_{\Gamma_1} \bar{u} \frac{\partial G}{\partial \mathbf{n}} d\Gamma_1, \quad (29)$$

where  $\alpha = 0.5$  if  $p \in \Gamma$ ,  $\alpha = 1$  if  $p \in \Omega$ , and  $\alpha = 0$  if  $p \notin \Omega$ . Equation (29) shows that potential at the point  $p$ , i.e.,  $u^p$ , can be computed as a sum of integrals over the boundaries  $\Gamma_1$  and  $\Gamma_2$ . This equation is the integral formulation of the Laplace equation and it is the base of the BEM for the Laplace equation.

Now, since we consider the case of homogeneous Neumann boundaries, i.e.,  $\bar{q} = \frac{\partial u}{\partial \mathbf{n}} = 0$ , the second integral of the right hand-side of equation (29) vanishes. Thus, to solve equation (29), integration over the *whole* boundary of  $\Omega$ , i.e.,  $\Gamma_1 \cup \Gamma_2$  is required. Solution procedure of (29) will be considered in the next subsection.

Nevertheless some improvement in solving (29) is possible. By demanding an extra condition for the fundamental solution  $G(p, q)$

$$\frac{\partial G(p, q)}{\partial \mathbf{n}} = 0 \quad \text{on} \quad \Gamma_1 \text{ and } \Gamma_2, \quad (30)$$

equation (29) is transformed into a simple equation:

$$\alpha u^p = \int_{\Gamma_1} q G(p, q) d\Gamma_1. \quad (31)$$

The important note about (31) is that it involves integration over the contact regions and not over the whole boundary. Green's function which satisfies (30) has been derived in [16] and incorporated into the advanced layout-to-circuit extractor SPACE [10] [5].

**4.0.2. Discretization and Solution** We will subdivide the boundary of substrate including the contacts into  $N$  elements which correspond to constant basis functions. It is possible to use elements which correspond to piecewise linear or quadratic basis functions. However these approaches are more complex from point of view of implementation, therefore we will not consider them in this report. Thus the values of  $u$  and  $\frac{\partial u}{\partial \mathbf{n}}$  are assumed to be constant over each element and equal to the value of the node which located in the middle of the element. The integral equation (29) can then be written for a given point  $p \in \Gamma$  as follows

$$\frac{u^p}{2} + \sum_{j=1}^N \int_{\Gamma_{2,j}} u \frac{\partial G(p, q)}{\partial \mathbf{n}} d\Gamma = \sum_{j=1}^N \int_{\Gamma_{1,j}} G(p, q) \frac{\partial u}{\partial \mathbf{n}} d\Gamma. \quad (32)$$

Since  $u$  and  $\frac{\partial u}{\partial \mathbf{n}}$  are constant over each element, they can be taken out from the integrals. Thus (32) takes the form

$$\frac{u^p}{2} + \sum_{j=1}^N \bar{H}^{pj} u^j = \sum_{j=1}^N K^{pj} q^j, \quad (33)$$

where

$$\bar{H}^{pj} = \int_{\Gamma_j} \sigma \frac{\partial G(p, q)}{\partial \mathbf{n}} d\Gamma, \quad K^{pj} = \int_{\Gamma_j} \sigma G(p, q) d\Gamma, \quad \text{and} \quad q = \frac{\partial u}{\partial \mathbf{n}}.$$

We can rewrite (33) in the more compact form

$$\sum_{j=1}^N H^{pj} u^j = \sum_{j=1}^N A^{pj} q^j, \quad (34)$$

where  $H^{pj} = \bar{H}^{pj}$  if  $i \neq j$  or  $H^{pj} = \bar{H}^{pj} + \frac{1}{2}$  if  $i = j$ . Thus (34) becomes a system of the form:

$$H\mathbf{U} = M\mathbf{Q}, \quad (35)$$

where  $H \in \mathbb{R}^{N \times N}$  and  $M \in \mathbb{R}^{N \times N}$ ,  $\mathbf{U} \in \mathbb{R}^N$  contains potentials at  $\Gamma_2$  and  $\mathbf{Q} \in \mathbb{R}^N$  contains current fluxes at  $\Gamma_1$ . Since at some nodes, values of  $u$  and  $\frac{\partial u}{\partial \mathbf{n}}$  are known from the boundary conditions, we rearrange the system of equations in such a way that all unknowns are on the left

side. The system will take the form

$$A\mathbf{X} = \mathbf{B}, \quad (36)$$

where  $X$  contains unknown values of  $u$  and  $\frac{\partial u}{\partial \mathbf{n}}$  on the boundary  $\Gamma$ . Solving this system of equations, one can obtain the values of  $u$  and  $\frac{\partial u}{\partial \mathbf{n}}$  at the boundary nodes where boundary conditions  $\bar{q}$  and  $\bar{u}$ , respectively, were specified. Once the system is solved, it is also possible to compute values of  $u$  and its derivatives at any point  $p$  inside of the domain  $\Omega$ . The values of  $u$ 's are computed at any internal point  $p$  using formula (29) which can be written as

$$u^p = \int_{\Gamma_1} \frac{\partial u}{\partial \mathbf{n}} G d\Gamma_1 - \int_{\Gamma_2} u \frac{\partial G}{\partial \mathbf{n}} d\Gamma_2. \quad (37)$$

The values of internal flux, for instance, in the direction  $x$ , i.e.,  $\frac{\partial u}{\partial x}$ , is calculated by carrying out derivative on (37), i.e.,

$$\left(\frac{\partial u}{\partial x}\right)_p = \int_{\Gamma_1} \frac{\partial u}{\partial x} \left(\frac{\partial G}{\partial x}\right)_p d\Gamma_1 - \int_{\Gamma_2} u \left(\frac{\partial G}{\partial x}\right)_p d\Gamma_2. \quad (38)$$

However for the sake of resistance extraction, it is not required to compute values of  $u$  and its derivatives at the points inside of the domain  $\Omega$ . The values of  $u$  and  $\frac{\partial u}{\partial \mathbf{n}}$  at the boundaries are only required which can be achieved by solving the system (36).

Note, that matrix  $A$  in (36) has the size of the number of boundary elements and it is dense, while in case of FEM discretization matrix  $Y$  in (22) is sparse and has the size of the number of interior nodes of the finite elements.

*4.0.3. Admittance matrix* In case of substrate modeling the goal is to obtain an admittance matrix which describes the behaviour of the substrate with respect to the contact areas. Here we will show how to construct such admittance matrix from the discretized equations obtained with BEM. This admittance matrix can be later interpreted as a resistance network. From (35) we obtain

$$\mathbf{Q} = M^{-1}H\mathbf{U},$$

where  $\mathbf{Q}$  collects all element current densities,  $\mathbf{U}$  collects all element potentials. The matrix

$$Y_e = M^{-1}H \quad (39)$$

denotes the admittance matrix between all boundary elements with respect to a virtual reference node, which represents potential at infinity.

Computing  $Y_e \in \mathbb{R}^{N \times N}$  requires solving  $N$  times a system of linear equations of the form  $M\mathbf{x} = \mathbf{h}_i$  for  $\mathbf{x}$ , where  $\mathbf{h}_i$  denotes the  $i$ -th column of  $H$  matrix. Using  $LU$  decomposition of  $M$ , an approximate complexity to compute  $Y_e$  is  $O(N^3) + NO(N^2)$ . However, using the windowing technique, which is based on the Schur inversion algorithm [16] [9] and takes into account only influences between boundary elements that are relatively close to each other, it is possible to compute an approximate inverse of  $M$  in only  $O(N)$  time.

To extract the admittance matrix for the contacts, we introduce an incidence matrix  $F \in \{1, -1, 0\}^{N \times N_c}$ , where  $N_c$  denotes the number of contacts, such that:

$$F_{ij} = \begin{cases} 1 & \text{if } i\text{th boundary element belongs to the } j\text{th contact} \\ 0 & \text{otherwise.} \end{cases}$$

Thus admittance matrix which represents the network between all contacts with respect to the virtual reference node becomes  $Y \in \mathbb{R}^{N_c \times N_c}$ :

$$Y = F^T Y_e F,$$

which is symmetric dense matrix with positive diagonal entries and negative off-diagonal entries. By eliminating the reference node, one obtains a conductance matrix of resistance network which contains path resistances between all the contacts.

4.0.4. *Example* Let two contacts be defined at the top of the substrate. Thus  $Y$  is a  $2 \times 2$  symmetric admittance matrix:

$$Y = \begin{pmatrix} y & -y_s \\ -y_s & y \end{pmatrix},$$

which corresponds to the network presented in Figure 4. Eliminating the reference node, we obtain a conductance matrix which describes the network between the contact:

$$G = \frac{1}{2} \begin{pmatrix} y + y_s & -y - y_s \\ -y - y_s & y + y_s \end{pmatrix}.$$

Thus, the path resistance between the contacts equals  $\frac{2}{y+y_s}$ .

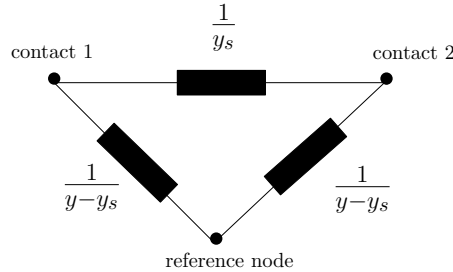


Figure 4. Resistor network with two substrate contacts and a reference node.

We note that there exists other way to compute the path resistance between the contacts. By setting  $\bar{u} = u_0$  at the left contact,  $\bar{u} = 0$  at the right contact, and solving the Laplace equation, the path resistance between the contacts can be computed as

$$R_t = \frac{u_0}{J_n} = \frac{u_0}{\sigma \sum_k l_k p_k},$$

where  $l_k$  denotes the length of the  $k$ th boundary element at the right contact and  $p_k$  denotes current flux flowing through the  $k$ th boundary element. In other words, to compute the path resistance between the contacts, one has to set initial potential  $u_0$  at one of the contact and ground another contact. By computing the current flux  $J_n$  through the second contact, the path resistance can be defined as a ratio  $\frac{u_0}{J_n}$ .

## 5. A 2D CASE STUDY

We will further compare the performance and characteristics of both methods, FEM and BEM, through the following example.

We consider a 2D substrate, in Figure 5,  $1000 \times 350 \mu m$  with two contacts  $10 \mu m$  in length at a distance of  $30 \mu m$  on the top the substrate. The conductivity of the substrate is  $10 S/m$ . A unite voltage was applied to the left contact, zero voltage was set at the right contact, and no current flow through non-contact areas, i.e.,  $\frac{\partial u}{\partial n} = 0$ .

If one is interested in getting to know values of potentials inside of the domain at many points, than FEM is the most suitable method because it discretizes the whole domain and solution is found at each discretization point. If one is only interested in the solution at the boundary, which is required, for instance, for extraction of resistance network, then BEM is excellent alternative. We will study the performance of BEM and FEM for extracting a resistance network for the substrate presented in Figure 5.

First, we solve the Laplace equation (10) with corresponding boundary conditions by FEM with very fine discretization over the whole domain. We obtain solution for potential presented in Figure 6. It can be seen that it contains a high voltage zone below the left contact and a low voltage zone around the second contact. The figure also includes current streamlines which show that the

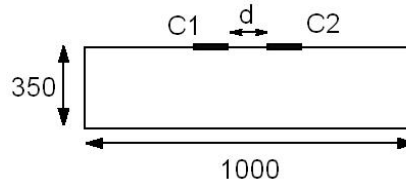


Figure 5. Substrate with two contacts C1 and C2, each of the size  $10\mu m$ . Distance values are in  $\mu m$ .

current flows from the left contact to the right one. Note, that conductivity  $\sigma$  does not influence on the behaviour of the potential but it influences on the normal component of the current  $J_n$ , going through the contacts:

$$\frac{J_n}{\sigma} = \frac{\partial u}{\partial \mathbf{n}}.$$

Second, we solve the Laplace equation (10) with corresponding boundary conditions by BEM implemented in Matlab [8]. We recall that for a 2D homogeneous domain, the Green's function has the form

$$G(p, q) = \frac{1}{2\pi} \ln \left( \frac{1}{r} \right).$$

Since the normal derivative of  $G(p, q)$  does not vanish on the boundary, the left sum of integrals in (32) cannot be neglected, and, therefore, we have to discretize the whole boundary of the substrate. The mesh at the contacts and between the contacts has been made finer than at the other parts of the substrate.

Figure 7 shows a comparison of BEM and FEM solutions for the potential on the upper side of the substrate, where contacts are located. To capture the behaviour of the potential by BEM, a coarse mesh at the boundaries was sufficient. From the figure we observe that both solutions by BEM and FEM coincide well.

In Figure 8 we show comparison of BEM and FEM solutions of the normal component of the current  $J_n$  at the top part of the substrate (at other parts current stays zero due to the boundary conditions). Due to the very sharp variations of the current at the contacts, we required a fine mesh for both BEM and FEM to obtain an agreement between the solutions. In general we observe that

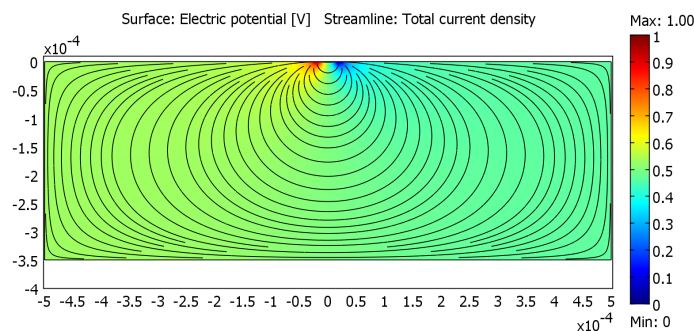


Figure 6. Potential distribution and streamlines of current in the 2D substrate

the potential does not require a very fine mesh for an adequate description, while current requires

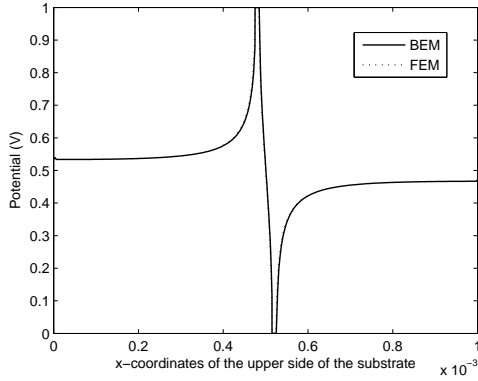


Figure 7. Potential at the upper boundary of the substrate.

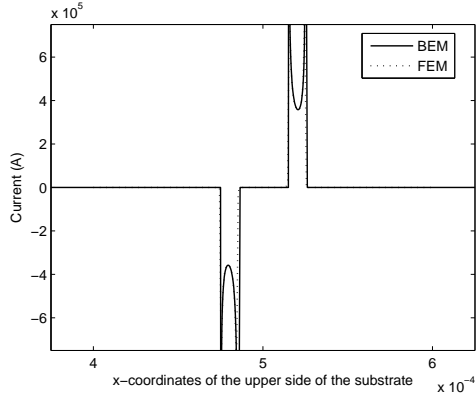


Figure 8. Solutions of current at the top boundary of the substrate by BEM and FEM.

fine discretization, especially close to the contacts. An accurate value of current at the boundary is crucial to determine the path resistance between the contacts.

Now we will proceed by analyzing the requirements of both methods (BEM and FEM) for having an accurate solution. To this extent, we use the following technique. We analyze the dependence of the computed value of the path resistance on the mesh size. When a mesh refinement conducts to a very small change in the resistance value, we can expect the solution to be mesh independent.

Figure 9 shows a relation between the number of FEM and BEM mesh elements and the computed value of the path resistance between the contacts. The number of mesh elements is directly related to the size of linear system to be solved for both cases. At this point, we should recall that the smaller matrix size for BEM does not necessarily implies faster computations than with FEM. From this plot we can notice that BEM requires a much smaller amount of elements than FEM for the computed value of path resistance to converge. This is, of course, due to the fact that BEM only requires to discretize the boundary, while FEM discretizes the whole 2D domain. Note, that we could not experience convergence of path resistance obtained by FEM with uniform refinement due to the lack of memory at the machine where computations were performed. To be able to compare the performance of BEM and FEM (with adaptive refinement) we measured the relative variation of path resistance based on the data of Figure 9. For instance, if further refinement provides a variation of path resistance, less than 1 %, then it means that we have reached two significant digits. This relative variation can be considered as a quality measure for the numerical solution. In Figure 10, we show a plot of the relative variation for the path resistance versus the computation time. It can be seen that solution computed with BEM converges at least five times faster than solution computed with FEM. For example, to achieve relative variation of path resistance of the order  $10^{-1}$ , BEM requires 0.66 sec., while FEM requires 3.7 sec.

Though BEM already performs better than FEM for extracting the resistance network of homogeneous substrate, there is a room for interesting improvements. Some possibilities are among the following.

As we mentioned before, one of the most important drawbacks of BEM is the fact that the discretized matrices in (35) are dense, and therefore computing inverse of  $M$  is expensive ( $O(n^3)$ ). However, the windowing technique [16][9], which is based on the Schur algorithm for approximate matrix inversion, can help to reduce complexity. The Schur algorithm requires the matrix  $M$  to be known only partly, in a staircase (band) around the main diagonal. The band structure corresponds to interactions between closely coupled boundary elements. The approximate inversion then implicitly estimates the entries of the matrix inside the band structure, such that the resulting  $M^{-1}$  contains zeros outside of the band structure.

Another important issue is the use of special Green's function [16] which satisfies:

$$\frac{\partial G(p, q)}{\partial \mathbf{n}} = 0 \quad \text{on} \quad \Gamma_1 \text{ and } \Gamma_2. \quad (40)$$

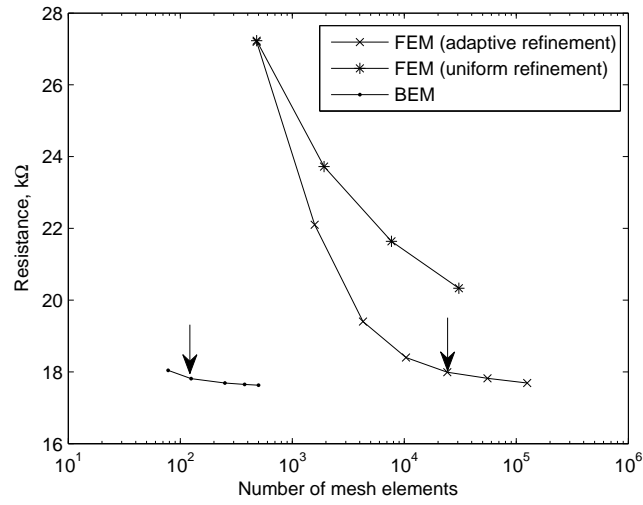


Figure 9. Dependence between resistance value and number of meshes. Vertical arrows indicate the points in which a further refinement will provide a relative variation of less than 1% in the path resistance value.

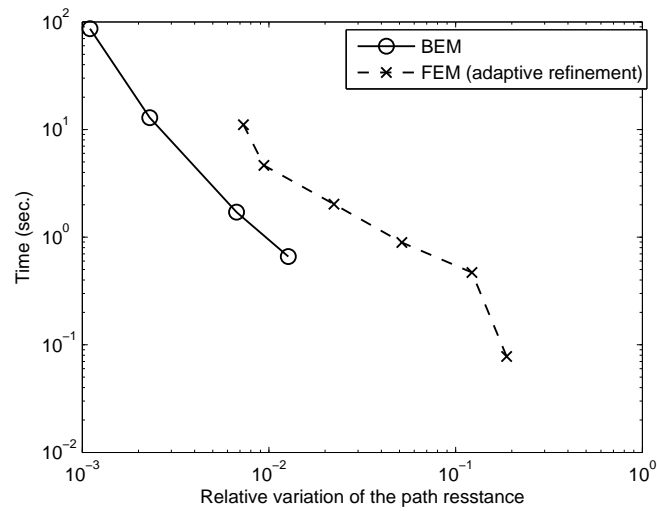


Figure 10. Dependence between the relative variations of path resistance and time.

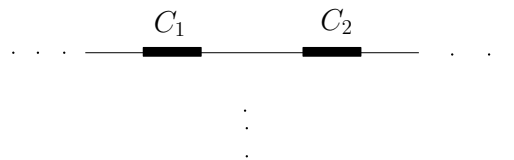


Figure 11. Semi-infinite substrate with two contacts.

The use of such Green's function results into necessity to integrate over the contact regions as in (31) and not over the whole boundary. This means that the substrate modeling is performed in semi-infinite domain as shown in Figure 11.

In the next section we consider extraction of a 3D homogeneous substrate and we will show how the above techniques influence on a solution obtained by BEM in comparison with to a solution obtained by FEM.

## 6. MODELING OF 3D SUBSTRATE BY BEM AND FEM

In this section we will compare the BEM and FEM methods for the simulation of a 3D homogeneous substrate. We discuss features of modeling the substrate by existing tools based on BEM and FEM and investigate the convergence of both methods.

We consider a uniformly doped (10 S/m) substrate  $1000 \times 1000 \times 380 \mu\text{m}$  which is presented in Figure 12. On the top layer it has two contacts of dimension  $5 \times 1.5 \mu\text{m}$ , and the distance between these contact is  $60 \mu\text{m}$ . To extract the equivalent resistance between two contacts, we will use the following modeling tools:

- SPACE [10] - layout-to-circuit extractor with implementation of BEM,
- Comsol [4] - FEM-based multiphysics modeling tool.

The technology data for BEM method can be described in SPACE through a high-level description language as described in [5]. Comsol is used through its graphical user interface.

### 6.1. Comparison between the methods

There are a few main differences between BEM and FEM. Substrate modeling by BEM implemented in SPACE requires discretization of only contact areas, while FEM discretizes the whole domain into tetrahedral elements. BEM assumes domain to be a semi-infinite half-space, while FEM requires finite domain. Therefore FEM can approximate BEM by defining the FEM domain as large as possible [14].

As for 2D case, extraction of the 3D substrate with two contacts by BEM leads to a resistance network with 3 nodes: two nodes correspond to the contacts (C1 and C2) and one node corresponds to a reference node SUB. After elimination of the reference node, the network can be compared to the one obtained by FEM which does not contain the reference node.

In Comsol we have chosen mesh with as much adaptive refinement as possible, given the available amount of memory in the machine on which Comsol runs. For SPACE we have used nominal extraction settings.

Table I demonstrates that the computed path resistances by BEM and FEM networks are close. The remaining differences between BEM and FEM results are caused by the fact that path resistance by FEM has not been yet converged to the final path resistance, while path resistance by BEM converges. This fact will be clarified in the next two sections. One can think that for a considered 3D substrate BEM does not approximate FEM well. This is not the case because the size of the contacts are small compared to the size of the substrate.

### 6.2. Convergence of FEM

This section presents practical study of the convergence of FEM by varying maximum mesh size at the contacts and total number of mesh elements.

We note that fine discretization of the contact areas is required to compute accurately extracted resistance. Indeed, the path resistance value,  $R$ , between the contacts depends on the value of current flux  $I$  through the first contact and applied voltage  $V$  at the second contact as

$$R = \frac{V}{I},$$



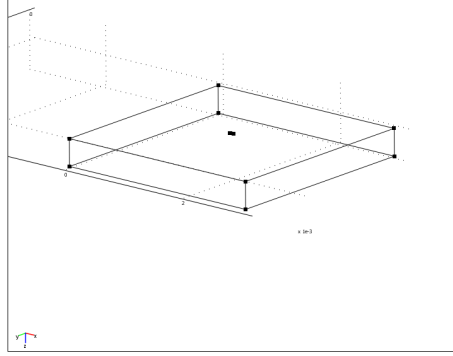


Figure 12. Example of the substrate with two contacts. Image taken from the Comsol user interface.

Table I. Resistance values in  $k\Omega$  extracted from the 3D substrate with two contacts. The bottom row indicates resistance between the contacts C1 and C2 after elimination of the reference node SUB

	BEM	FEM
R(C1,C2)	854.54	33.81
R(C1,SUB)	15.12	-
R(C1,SUB)	15.12	-
	29.22	33.81

Table II. Statistics about solutions by FEM with adaptive mesh refinement

# meshes at C1	112	136	358
# meshes (total)	28066	94753	178190
path resistance ( $k\Omega$ )	38.74	36.09	33.81
time (s)	6	73.6	218.4

The current flux requires computing the integral over the boundary of the contact area:  $I = \oint_{\Gamma} J_n dl$ , therefore discretization plays an important role. The finer discretization, the more accurate resistance value can be obtained.

Table II shows that adaptive mesh refinement makes the resistance value decreased. However comparing the last value of path resistance (33.81  $k\Omega$ ) with the previous one (36.09  $k\Omega$ ) shows that the convergence has not been achieved yet. Further refinement was not possible due to the lack of memory. From this we conclude that extraction of the substrate by FEM requires either smaller substrate's domain or more computer memory to perform further refinements.

### 6.3. Convergence of BEM

In this section we study convergence of BEM through the parameters available in the layout-to-circuit extractor SPACE. For this we choose nominal settings, and vary only individual parameters, while keeping other parameters at their nominal settings. The nominal settings are

- number of BEM meshes per contact = 68,
- size of BEM window =  $\infty$ , i.e., all entries of  $M^{-1}$  in (39) are taken into account.

Table III. Extraction statistics and resistance values for increasing refinement in the BEM mesh

#BEM elements	time (s)	mem (Mb)	$R (k\Omega)$
4	2	0.12	30.77
8	2	0.13	30.76
16	2	0.18	30.45
68	2.1	1.05	29.22
296	4.3	16.6	29.01
332	5	20.85	29.00

Table IV. Extraction statistics and resistance values for increasing size of the BEM window

BEM window size ( $\mu m$ )	time (s)	mem (Mb)	$R (k\Omega)$
1	2.1	0.188	25.58
5	2.1	0.370	29.73
30	2.3	0.408	29.73
50	2.3	1.057	29.22
$\infty$	2.3	1.057	29.22

6.3.1. *BEM mesh* The initial BEM mesh consists of 68 BEM elements per contact. Table III demonstrates that refinement has very little influence on resistance value between the contacts while it is relatively costly with respect to extraction time and memory usage.

6.3.2. *Size of BEM window* SPACE allows sparsification through the windowing technique [14][16] which can make the method more efficient at the cost of some accuracy. Table IV shows that windows's size has little influence on the resistance value, while memory usage increases if window's size increases. Changes in time are less noticeable due to the relatively small amount of contacts and meshes at each contact.

## 7. CONCLUDING REMARKS

In this report we have considered the problem of homogeneous substrate modeling by the boundary element method (BEM) and the finite element method (FEM). Depending on the characteristics of the particular task, BEM and FEM techniques have advantages and disadvantages. BEM finds the solution on the boundary, and to know the solution at some internal points, BEM requires postprocessing. On the other hand, FEM finds solution at each discretization point of the domain. Therefore, if one is interested in behaviour of the whole domain FEM is more suitable for this task. For other problem BEM proves to be a much better alternative.

For instance, for extraction of a resistance network which describes the behaviour of a homogeneous substrate, one requires to know the solution only at the contact areas. From this perspective, BEM is more attractive, since solutions at the inner nodes are not required and, therefore, we spare time and do not capture details which are not necessary. In this sense BEM is a model order reduction technique on the operator level. Furthermore, there is another aspect to consider. Solving a 3D problem by FEM may be time and memory-consuming due to necessity of fine discretization, while BEM is out of this problem.

As we saw, BEM relies on the Green's function and requires discretization of the whole boundary. We have explored the usage of BEM for modeling of 2D and 3D substrates. A special choice of Green's function leads that only contact areas have to be discretized and not the whole boundary. In this case BEM considers substrate as a semi-infinite half space. As a result, FEM solution at the contacts can approximate BEM solution by making FEM domain as large as possible.

BEM leads to dense matrices, which have the size of the number of elements at the boundary. Therefore, we also addressed the problem of BEM delivering dense matrices. One of the alternative we studied was the use of windowing technique which sparsifies the matrix by taking into account only influences between boundary elements that are relatively close to each other. We have observed that sparsification has little influence on the quality of extraction.

We note that the class of problems in which BEM can be applied is limited. For example, modeling of substrates involving layout-dependent doping patterns is more challenging than modeling of homogeneous substrates [15][14]. In this case, finding analytical Green's function becomes extremely difficult, which restricts the kind of problems in which BEM can be applied efficiently. To overcome this problem, FEM or combined BEM/FEM methods can be considered. Nonetheless, BEM performs better than FEM when applied to homogeneous substrate extraction.

#### ACKNOWLEDGEMENTS

The first author would like to thank S. de Graaf and N.P. van der Meijs for the help with the layout-to-circuit extractor SPACE, and P.I. Rosen Esquivel and J. Rommes for the useful discussions.

#### REFERENCES

1. R. Achar and M. S. Nakhla. Simulation of High-Speed Interconnects. In *Proc. of the IEEE*, pages 693–728, 2001.
2. E. Barke. Resistance calculations from mask artwork data by finite element method. In *Proc. 22nd Design Automation Conference*, pages 305–311, 1985.
3. C. A. Brebbia and J. Dominguez. *Boundary Elements. An Introductory Course*. Computational Mechanics Publications, 1989.
4. Comsol. Comsol multiphysics ver. 3.4, <http://www.comsol.com>, september 2010.
5. A. J. van Genderen, N. P. van der Meijs, and T. Smedes. Space substrate resistance extraction user's manual. Report et-ns 96-03, Delft University of Technology, 2006.
6. A.J. van Genderen. *Reduced Models for the Behavior of VLSI Circuits*. PhD thesis, Delft University of Technology, Delft, 1991.
7. H.C. de Graaf and F.M. Klaassen. *Compact Modeling for Circuit Design*. Springer Verlag, 1990.
8. Mathworks. MATLAB ver. 7.5.0.338, <http://www.mathworks.com>, april 2010.
9. N. P. van der Meijs. *Accurate and Efficient Extraction*. PhD thesis, Delft University of Technology, 1992.
10. N. P. van der Meijs, A. J. van Genderen, F. Beefrink, and P. J. H. Elias. Space user's manual. Report et-nt 92.21, Delft University of Technology, 2005.
11. C. R. Paul, K. W. Whites, and S. A. Nasar. *Introduction to Electromagnetic Fields*. WCB/McGraw-Hill, 1998.
12. A.C. Polycarpou. *Introduction to the Finite Element Method in Electromagnetics*. Morgan & Claypool, 2006.
13. A. E. Ruehli and A. C. Cangellaris. Progress in the Methodologies for the Electrical Modeling of Interconnects and Electronic Packages. *Proceedings of the IEEE*, 89(5):740–771, 2001.
14. E. Schrik. *A combined BEM/FEM Method for IC Substrate Modeling*. PhD thesis, Delft University of Technology, Delft, 2006.
15. E. Schrik and N. P. van der Meijs. Combined BEM/FEM Substrate Resistance Modeling. In *Proceedings of the 39th Design Automation Conference*, pages 771–776. New Orleans, LA, August 2002.
16. T. Smedes, N.P. van der Meijs, and A.J. van Genderen. Boundary element methods for 2D capacitance and substrate resistance calculations in inhomogeneous media in a vlsi layout verification package. *Advances in Engineering Software*, 20:19–27, 1994.
17. M. Zahn. *Electromagnetic Field Theory: a problem solving approach*. John Wiley & Sons, New York, Chichester, Brisbane, Toronto, 1979.

## PREVIOUS PUBLICATIONS IN THIS SERIES:

Number	Author(s)	Title	Month
II-04	M.E. Hochstenbach A. Muhič B. Plestenjak	On linearizations of the quadratic two-parameter eigenvalue problems	Jan. '11
II-05	R. Ionutiu J. Rommes W.H.A. Schilders	SparseRC: sparsity preserving model reduction for RC circuits with many terminals	Jan. '11
II-06	M.E. Hochstenbach L. Reichel	Fractional Tikhonov regularization for linear discrete ill-posed problems	Jan. '11
II-07	W. Hoitinga E.H. van Brummelen	A discontinuous Galerkin finite-element method for a 1D prototype of the Boltzmann equation	Jan. '11
II-08	M.V. Ugryumova W.H.A. Schilders	Evaluation and comparison of FEM and BEM for extraction of homogeneous substrates	Febr. '11